

Self-Assembly of *n*-Alkyl Thiols as Disulfides on Au(111)

P. Fenter,* A. Eberhardt, P. Eisenberger

A grazing incidence x-ray diffraction study of $\text{CH}_3(\text{CH}_2)_9\text{SH}$ self-assembled on the (111) surface of gold revealed a disulfide head group structure, which provides a context in which to understand the structure and self-assembly process of this widely studied system. The structure consists of a nearly hexagonal two-dimensional arrangement of the hydrocarbon chains with a dimerization of the sulfur head groups (accommodated through a gauche bond), resulting in a S-S spacing of 2.2 angstroms. These results demonstrate the importance of internal molecular degrees of freedom in the templating of "soft" organic materials on inorganic substrates.

Self-assembled monolayers (SAMs) have attracted considerable attention as a model system for many fundamental and technological phenomena (for example, supramolecular assembly, wetting, tribology, and corrosion inhibition) because of both their simplicity and stability (1–3). In particular, SAMs consisting of *n*-alkane thiols adsorbed on Au(111) have been extensively studied (1, 4–10). Surprisingly, even in this widely studied system, there is little that is directly known about the head group–substrate structure and interaction. Previous studies found that long-chain disulfides and thiols form similar films when grown from solution, and there is strong evidence that the final chemisorbed state of the molecules is the same in these two cases (11). Although we are unaware of any measurements that have in fact determined the structure of the sulfur–substrate bond, a general consensus in the literature has been reached that the bonding state is in the form of an Au-thiolate (1, 11–13).

We performed an in-depth x-ray diffraction study of the $\text{CH}_3(\text{CH}_2)_9\text{SH}$ (C10) monolayer on Au(111) and found that the results are inconsistent with the generally accepted thiolate bonding structure. The equilibrium structure of the monolayer includes a S-S spacing of 2.2 Å, which strongly implies the existence of a S–S bond. These results demonstrate that internal molecular conformations are an intrinsic component of even these relatively simple SAM systems. Such a quantitative structural understanding is critical to the control and design of more complex molecular assemblies, as well as in developing a general understanding of organic–inorganic interfaces.

These measurements were performed on the Exxon X10A beamline at the National Synchrotron Light Source (NSLS) with the use of a z -axis spectrometer with a wavelength of 1.09 Å and an incident angle of

1° . The resolution was set to $\Delta Q_{\parallel} = 0.21 \text{ \AA}^{-1}$ and $\Delta Q_z = 0.041 \text{ \AA}^{-1}$, and the data have been normalized to remove resolution effects (14, 15); for convenience, the hexagonal peak intensity has been divided by 3 to account for the multiplicity of $C(4 \times 2)$ domains with respect to the hexagonal substrate. The samples were prepared by growth in dilute ($\sim 1 \text{ mM}$) solutions of thiol in ethanol as described previously and were annealed in vacuum to remove any disorder that was a result of the self-assembly process (15, 16). The average domain size of the resulting film was $>400 \text{ \AA}$, and consequently, these results reflect the intrinsic equilibrium structure of these films.

In Fig. 1, we show a map of the diffraction intensities for the C10 monolayer as a function of Miller indices h and k (for $Q_z \approx 0$). In this representation, the (1,1), (0,2), and related "hexagonal" peaks coincide with the previously observed $\sqrt{3} \times \sqrt{3}R30^\circ$ structure, whereas the other peaks [for example, $(\frac{1}{2},0)$, $(\frac{1}{2},1)$, and $(\frac{3}{2},0)$] have been notated as a $C(4 \times 2)$ unit cell, which was first observed by He atom diffraction (17) and subsequently by x-ray diffraction (15) and scanning tunneling microscopy (STM) (10). Although the $C(4 \times 2)$ unit mesh is commensurate with the smaller $\sqrt{3} \times \sqrt{3}R30^\circ$ structure, its size implies that there can be as many as four inequivalent molecules in the monolayer. It is notable that there appear to be systematic absences in the diffraction pattern; that is, the (1,0), (0,1), (1,2), and (0,3) peaks are either missing or less than 1/15 the strength of the other superlattice peaks [in fact, this symmetry appears to be exact for monolayers of $\text{CH}_3(\text{CH}_2)_{17}\text{SH}$ (C18) on Au(111) (14)]. This pattern of absences is characteristic of a centered rectangular cell and implies both the equivalence of molecules 1 and 2 (as well as molecules 3 and 4) and a relative displacement of $(a/2)(x + \sqrt{3}y)$ between these symmetry equivalent molecules (x and y are the unit vectors in the x and y directions, respectively, and a is the lattice parameter of the $\sqrt{3} \times \sqrt{3}R30^\circ$

lattice). Consequently, there are only two inequivalent molecules in the unit cell. These systematic absences also allow us to rule out any other $C(4 \times 2)$ structures that do not exhibit this centered rectangular symmetry.

One can obtain additional structural information by examining the Q_z dependence of each of the diffraction peaks (that is, the surface Bragg rods) (Fig. 2). It is immediately clear from these data that although the superlattice peaks generally exhibit a rather flat intensity profile (characteristic of an interface), the hexagonal rods exhibit, in addition, a strong modulation, which we have previously found to be the molecular form factor of the hydrocarbon chain (and which contains information about the orientation of the hydrocarbon chain) (15). The lack of modulation in the superlattice data immediately implies that these data are not primarily the result of an ordering of the hydrocarbon chains (for example, a herringbone structure), as has been previously assumed, but instead, the structure must contain displacements of the S head group or the Au surface atoms (that is, a complex

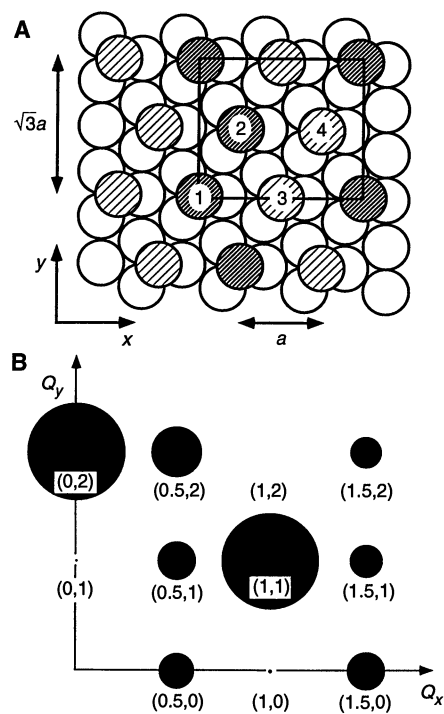


Fig. 1. (A) A schematic of the $C(4 \times 2)$ unit cell, indicating Au surface atoms (open circles) and thiol molecules (shaded circles); shading denotes equivalent thiol molecules, as derived from the symmetry of the diffraction pattern. (B) Intensity map for a single domain of the C10 monolayer; the size of the circles are proportional to the integrated peak intensities for each peak measured at $Q_z \approx 0.1 \text{ \AA}^{-1}$. The (1,1) and (0,2) peaks have been divided by 3 so that the intensities can be compared with a single domain of the $C(4 \times 2)$ unit cell.

Department of Physics and Princeton Materials Institute, Princeton University, Princeton, NJ 08540, USA.

*To whom correspondence should be addressed.

interface structure). This structure is further supported by our observation that the Bragg rod profiles for the superlattice peaks are very similar for the C10 and C18 monolayers (14), even though their hydrocarbon structures are different (15).

To test these observations, we compared the data to rigorous intensity calculations using the generally accepted structural model of these films (1, 7), in which an all-trans thiol molecule is assumed, with the S head group bound at the threefold hollow site of Au(111), and we optimized the fit by varying the tilt angle, tilt direction, and twist (about the hydrocarbon chain axis) of the thiol molecules, as well as relaxations in the Au surface (including a lateral trimerization about the S site and vertical relaxations of the top two Au layers). In spite of this large number of structural parameters, we cannot achieve an acceptable fit (Fig. 2) (the quality of fit, $S\chi^2 = 114$, is defined as $S\chi^2 = (1/n)\sum[(I_{\text{exp}} - I_{\text{calc}})/\sigma I_{\text{exp}}]^2$, where the sum is over the n data points and σI_{exp} is the statistical uncertainty in the experimental intensity I_{exp}). If we relax the requirement of a threefold hollow bonding site and include relaxations in the Au surface consistent with the $C(4 \times 2)$ symmetry, the quality of fit is still poor ($S\chi^2 = 16$) and cannot be significantly improved, even

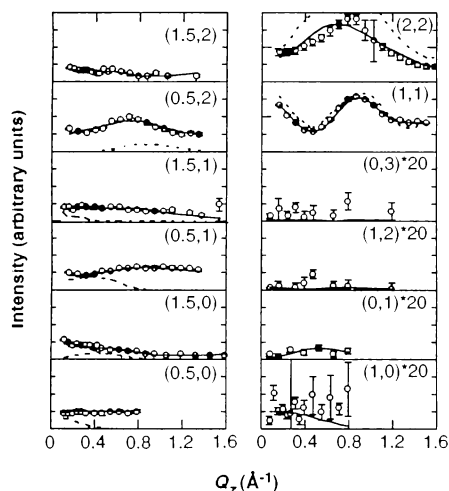


Fig. 2. The Q_z dependence of each of the diffraction peaks of the $C(4 \times 2)$ unit cell for C10 on Au(111). The data are shown on the same vertical scale, except for the "forbidden" superlattice peaks, which have been multiplied by a factor of 20, and the "hexagonal" peaks, which have been divided by a factor of 3, as in Fig. 1. Structure factor calculations were fit to the data and include the positions and (isotropic) vibrational amplitudes of the S, C, and Au atoms in the unit cell. The solid (dashed) line is the calculation of the disulfide (thiolate) structure. The disulfide model includes a S-S spacing of $d_{\text{SS}} = 2.2 \text{ \AA}$ and a tilt angle of the hydrocarbon chain of $\theta_t = 37^\circ$ in a direction $\chi = 21.8^\circ$ away from the NNN tilt direction.

if we allow unphysical hydrocarbon chain spacings ($< 4 \text{ \AA}$) and unusually large vibrational amplitudes ($> 1 \text{ \AA}$).

To determine the essential element of the $C(4 \times 2)$ structure, we compared the relative experimental intensities to simple analytical expressions for the scattering intensity $I(Q) = |\sum f_i \exp(iQr_i)|^2$, where f_i is the atomic scattering factor for an atom located at r_i . If the $C(4 \times 2)$ structure is thought of as a distortion of a $\sqrt{3} \times \sqrt{3}R30^\circ$ lattice (as it can be without any loss of generality), then the intensity of the superlattice peaks is expected to vary as $\sin^2[Q(\delta_1 - \delta_3)/2]$, where $Q = 1.257 \text{ \AA}^{-1}(h^2 + k^2/3)^{1/2}$ is the magnitude of the momentum transfer and δ_i is the typical size of a structural distortion away from the $\sqrt{3} \times \sqrt{3}R30^\circ$ lattice for molecule i . For instance, from the lack of a hydrocarbon form factor in the superlattice peaks, we can estimate an upper limit on the displacements of the hydrocarbon chain away from the hexagonal lattice, δ_{hyd} , for which we find $\delta_{\text{hyd}} < 0.1 \text{ \AA}$. Similarly, we can show that the Au surface atoms may be laterally relaxed by as much as $\delta_{\text{Au}} \approx 0.05 \text{ \AA}$ but that this small relaxation will result in a $(Q\delta)^2$ dependence of the intensity, which does not fully explain the data. Similarly, if we allow the S head groups to dimerize, we find that this can explain the observed diffraction intensities, given an average lateral distortion of $\delta_s = (\delta_1 - \delta_3)/2 \approx 1.4 \text{ \AA}$. This is surprising because the distance of the S head group from the hydrocarbon axis of an all-trans thiol molecule is only $\sim 0.6 \text{ \AA}$. Consequently, we can infer that the diffraction data are inconsistent with an all-trans molecular structure.

The simplest model of the internal molecular structure that is consistent with a large displacement of the S head groups is one in which the S-C bond is gauche (Fig. 3); this results in a distance of $\sim 2 \text{ \AA}$ between the S head group and the hydrocarbon axis. When we include this internal molecular structure in the intensity calculations, we obtain excellent agreement between the data and the calculation ($S\chi^2 = 1.9$) with a S-S distance [between molecules 1 and 3 (Fig. 1)] of $d_{\text{SS}} = 2.2 \text{ \AA}$ (we believe that the error in this quantity is dominated by systematic error and estimate the uncertainty to be about $\pm 0.2 \text{ \AA}$), and the hydrocarbon chains remain in a nearly hexagonal two-dimensional packing. This result is striking because it falls between the equilibrium S-S bond distance in many sulfur compounds ($\sim 2.0 \text{ \AA}$) (18) and the somewhat larger value ($\sim 2.5 \text{ \AA}$) observed for a sulfur layer on Au(111) under electrochemical control (19). Our structural results therefore imply that there exists a bond between pairs of S head groups, which directly leads to the interpretation that the

equilibrium structure of the molecule is in the form of a disulfide (Fig. 3). Because our data set is not large enough to determine the detailed internal structure of the molecules, we propose this structure as the simplest model consistent with the observed sulfur dimerization. Consequently, we expect that although our description of the internal molecular structure (especially near the head group) contains the essential elements of the structure, it may be incomplete.

From the present data, we find an optimal fit when the two S head groups occupy inequivalent bonding sites on the Au surface, with one S located approximately in the Au threefold hollow site and the other S located near the Au bridge site. We expect that this inequivalence in binding sites should result in an observable splitting of the sulfur core levels as might be measured in x-ray photoelectron spectroscopy measurements (11, 12, 20). The structural analysis also results in an optimal tilt angle and tilt direction of $\theta_t = 37.0 \pm 0.5^\circ$, $\chi = 21.8 \pm 0.6^\circ$ [with respect to the next nearest neighbor (NNN) direction].

Although our results contradict the currently accepted picture of the thiolate bonding structure, we are unaware of any unambiguous evidence in the literature that demonstrates that the bonding state of these long chain monolayers is in the form of a thiolate (1, 11-13). Although electron diffraction studies have found a simple $\sqrt{3} \times \sqrt{3}R30^\circ$ structure for CH_3SH monolayers (which implies a thiolate bond-

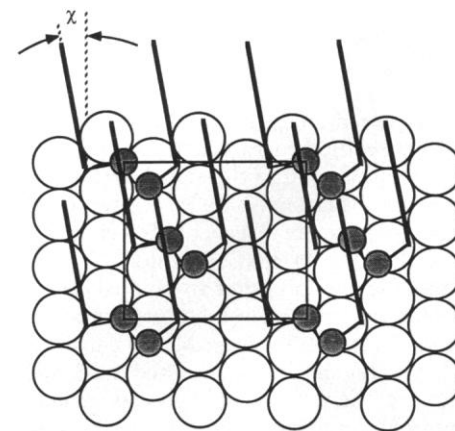


Fig. 3. A schematic of the proposed structure of C10-Au(111). Sulfur atoms, hydrocarbon chains, and Au atoms are indicated by shaded circles, solid lines, and open circles, respectively (the gauche defect at the S-C bond is indicated by the offset of the S head group from the hydrocarbon chain). The four molecules in the unit cell are shown (with the unit cell boundaries noted). Notice that the introduction of a gauche defect at the S-C bond allows the hydrocarbon packing to be hexagonal, whereas the S-S spacing is dimerized with a spacing of $d_{\text{SS}} = 2.2 \text{ \AA}$.

ing), we do not believe that this is in any way contradictory because we have previously demonstrated that the structure of the monolayers depends on the chain length; in the limit of small chain lengths, the structure should be dominated by the interface, which would be expected to result in a simple $\sqrt{3} \times \sqrt{3}R30^\circ$ structure. Furthermore, a recent theoretical calculation has found that the adsorption process [that is, a thiol forming a thiolate on Au(111) and releasing hydrogen in the form of H_2] may be endothermic by a few kilocalories per mole (7) and may consequently argue against the thiolate structure.

Recent STM results [which find a $C(4 \times 2)$ unit cell] find an apparent height modulation of symmetry-inequivalent molecules that are hexagonally packed lateral to the surface (10). This is fully consistent with our derived structure and may be caused by both the inequivalent sulfur bonding sites as well as the different twists of the hydrocarbon chains about the chain axis. A detailed comparison of the x-ray and STM results may provide a unique opportunity to understand the tunneling mechanism in these films. A height modulation of the hydrocarbon chains may also explain the sensitivity of He atom diffraction to the $C(4 \times 2)$ structure (17), even though He atom diffraction does not directly probe the monolayer-substrate interface. Finally, we expect that nature of the bonding to the substrate may explain the discrepancy between the greater thermal stability and lack of rotator phases in our previously observed (15) experimental phase behavior, as compared to both the predicted monolayer (8) and the known bulk *n*-alkane phase behaviors (21).

These results imply an entirely new context in which to view the self-assembly of these materials. In particular, previous results on the structure, defects, molecular diffusion, as well as the self-assembly process itself may need to be reinterpreted. The presence of a gauche defect at the S-C bond is at first surprising. Yet, because the energy cost of an isolated gauche defect is comparable to thermal energies (22), there will be a significant density of gauche bonds for an isolated molecule. Clearly, the self-assembly process includes internal conformational changes to form a dense layer consisting of extended hydrocarbon chains, and it is not difficult to imagine that gauche defects that reduce the steric or bonding constraints in these complex systems may be readily accommodated.

The resulting difference between the head group and hydrocarbon chain spacings provides a simple illustration of the structural versatility in these systems. This highlights the importance of both conformation-

al degrees of freedom and the impact of the interface on the film structure, which may result in both novel structures and growth modes. It also raises the possibility of using internal molecular degrees of freedom (for example, conformations) within supramolecular assemblies and in the epitaxy of wide classes of "soft-soft" and "soft-hard" growth systems [such as organic quantum well structures (23) and the bio-mineral interface (24), respectively] as a means to reduce or eliminate the need for lattice matching in these systems.

REFERENCES AND NOTES

1. L. H. Dubois and R. G. Nuzzo, *Annu. Rev. Phys. Chem.* **43**, 437 (1992).
2. J. D. Swalen *et al.*, *Langmuir* **3**, 932 (1987).
3. A. Ulman, *An Introduction to Ultrathin Organic Films* (Academic Press, San Diego, CA, 1991).
4. N. Camillone III, C. E. D. Chidsey, G.-Y. Liu, T. M. Putvinski, G. Scoles, *J. Chem. Phys.* **94**, 8493 (1991).
5. L. H. Dubois, B. R. Zegarski, R. G. Nuzzo, *ibid.* **98**, 678 (1993).
6. R. G. Nuzzo, L. H. Dubois, D. L. Allara, *J. Am. Chem. Soc.* **112**, 558 (1990).
7. H. Sellers, *Surf. Sci.* **294**, 99 (1993).
8. J. Hautman and M. L. Klein, *J. Chem. Phys.* **93**, 7483 (1990).
9. C. D. Bain *et al.*, *J. Am. Chem. Soc.* **111**, 321 (1989).

10. G. E. Poirier and M. J. Tarlov, *Langmuir* **10**, 2853 (1994).
11. C. D. Bain, H. A. Biebuyck, G. M. Whitesides, *ibid.* **5**, 723 (1989).
12. R. G. Nuzzo, B. R. Zegarski, L. H. Dubois, *J. Am. Chem. Soc.* **109**, 733 (1987).
13. H. A. Biebuyck and G. M. Whitesides, *Langmuir* **9**, 1766 (1993).
14. P. Fenter *et al.*, unpublished results.
15. P. Fenter, P. Eisenberger, K. S. Liang, *Phys. Rev. Lett.* **70**, 2447 (1993).
16. N. Camillone III *et al.*, *J. Chem. Phys.* **99**, 744 (1993).
17. N. Camillone III, C. E. D. Chidsey, G.-Y. Liu, G. Scoles, *ibid.* **98**, 3503 (1993).
18. B. Beagley and K. T. McAloon, *Trans. Faraday Soc.* **67**, 3216 (1971).
19. X. Gao, Y. Zhang, M. J. Weaver, *J. Phys. Chem.* **96**, 4156 (1992).
20. R. G. Nuzzo, F. A. Fusco, D. L. Allara, *J. Am. Chem. Soc.* **109**, 2358 (1987).
21. D. M. Small, *The Physical Chemistry of Lipids: From Alkanes to Phospholipids* (Plenum, New York, 1986).
22. J. F. Nagle, *Faraday Discuss. Chem. Soc.* **81**, 151 (1986).
23. F. F. So, S. R. Forrest, Y. Q. Shi, W. H. Steier, *Appl. Phys. Lett.* **56**, 674 (1990).
24. S. Mann *et al.*, *Science* **261**, 1286 (1993).
25. We acknowledge the close interaction with J. Li, N. Camillone III, G.-Y. Liu, T. A. Ramanarayanan, C. E. D. Chidsey, G. Scoles, and K. Liang throughout these studies. This work is supported by National Science Foundation award DMR-9311871 and was performed at the NSLS, which is supported by Department of Energy contract DE-AC0276CH-00016.

27 June 1994; accepted 7 September 1994

Growth and Sintering of Fullerene Nanotubes

D. T. Colbert, J. Zhang, S. M. McClure, P. Nikolaev, Z. Chen, J. H. Hafner, D. W. Owens, P. G. Kotula, C. B. Carter, J. H. Weaver, A. G. Rinzler, R. E. Smalley*

Carbon nanotubes produced in arcs have been found to have the form of multiwalled fullerenes, at least over short lengths. Sintering of the tubes to each other is the predominant source of defects that limit the utility of these otherwise perfect fullerene structures. The use of a water-cooled copper cathode minimized such defects, permitting nanotubes longer than 40 micrometers to be attached to macroscopic electrodes and extracted from the bulk deposit. A detailed mechanism that features the high electric field at (and field-emission from) open nanotube tips exposed to the arc plasma, and consequent positive feedback effects from the neutral gas and plasma, is proposed for tube growth in such arcs.

In 1991 Iijima (1) discovered that micrometer lengths of a multiwalled, somewhat imperfect version of tubular fullerenes were present in the same sort of carbon arc apparatus already used to make C_{60} and other small, spheroidal fullerenes. Much progress has been made in increasing the

yield of such nanotubes (2) and in purification (3, 4), but substantial quantities of carbon nanotubes are still not generally available with a perfect graphene structure over sufficient lengths that they truly deserve the term fullerene tubes (5) or fibers. The studies reported below show that sintering of adjacent nanotubes to each other due to the high-temperature conditions of growth is the principal cause of defects in nanotubes produced in arcs. We have uncovered striking new clues of why nanotubes grow in such abundance in such arcs, and present a detailed mechanistic model for this growth.

Following on the initial work by Ebbesen and Ajayan (2), our first study of carbon

D. T. Colbert, J. Zhang, S. M. McClure, P. Nikolaev, Z. Chen, J. H. Hafner, A. G. Rinzler, R. E. Smalley, Rice Quantum Institute and the Departments of Chemistry and Physics, M.S. 100, Rice University, P.O. Box 1892, Houston, TX 77251, USA.

D. W. Owens, P. G. Kotula, C. B. Carter, J. H. Weaver, Electronic Materials Group, Department of Chemical Engineering and Materials Science, University of Minnesota, 421 Washington Avenue, S.E., Minneapolis, MN 55455, USA.

*To whom correspondence should be addressed.